Application of a widely electrically tunable diode laser to chemical gas sensing with quartz-enhanced photoacoustic spectroscopy

Damien Weidmann, Anatoliy A. Kosterev, and Frank K. Tittel
Rice Quantum Institute, Rice University, Houston, Texas 77251-1892

Neil Ryan and David McDonald
Intune Technologies, Park West, Dublin 12, Ireland

Received February 3, 2004

A near-infrared diode laser with sample-grating distributed Bragg reflectors was used as a widely tunable spectroscopic source for multispecies chemical sensing. Quartz-enhanced photoacoustic spectroscopy was utilized to obtain high absorption sensitivity in a compact gas cell. CO_2, H_2O, C_2H_2, and NH_3 were monitored. A noise equivalent sensitivity of 8×10^{-9} cm^{-1} W^{-1} $Hz^{-1/2}$ for NH_3 detection was achieved, which corresponds to a NH_3 mixing ratio of 4.4 parts in 10^6 by volume (ppmv) with a 1-s time constant and available 5.2-mW optical power in the gas cell. © 2004 Optical Society of America

OCIS codes: 140.5960, 280.3420, 300.6430, 300.6320.

Recent developments in telecommunication laser sources have resulted in near-infrared diode lasers that are tunable over a range of 40–100 nm.[1] These sources have created new opportunities for spectroscopic gas sensing because widely tunable lasers permit multispecies gas monitoring[2] and can also be applied to the detection of broadband absorbers. We combined a widely tunable diode laser module (Intune Technologies AltoWave3500) with recently introduced quartz-enhanced photoacoustic spectroscopy[3] (QEPAS) to demonstrate multispecies chemical sensing.

The widely tunable diode laser design used in this study relies on sample-grating distributed Bragg reflector (SG-DBR) technology.[4] The laser chip is composed of a rear Bragg reflector, a phase section, a gain section, and a front Bragg reflector. The refractive indices of these four sections can be independently adjusted by carrier injection. Depending on these four parameters and the laser chip temperature, mode cartography is performed for subsequent computer-based user access to a specific wavelength.[5] Unlike external cavity technology, the SG-DBR technology permits a fast wavelength switching time (<10 μs).

The integrated laser-controller module covers the 1525–1570-nm spectral range as shown in Fig. 1, with a side-mode suppression ratio of better than 40 dB. The tuning is not truly continuous, but the proper selection of currents through the laser regions mentioned above establishes a 30-GHz window of continuous tunability (channel) anywhere in this range. As many as 255 user-specified laser channels can be stored in the module memory with a central channel frequency precision of better than ± 2 GHz. Module dimensions are 100 mm $\times$ 72 mm $\times$ 13 mm, and the laser output is coupled to a single-mode polarization-maintaining fiber. One selects a channel by sending a command to the module via an RS232 interface. In a given channel, one can modulate the laser wavelength at a frequency of as much as 50 kHz in a ± 15-GHz optical frequency range by applying an external voltage to the laser module's analog modulation input. The corresponding residual amplitude modulation is virtually absent, because the current through the laser gain region does not change. Nineteen channels were programmed for access to absorption lines of CO_2, H_2O, C_2H_2, NH_3, CO, OH, and HCN. The first four species listed were monitored in the research reported here. The characteristics of the laser channels and the corresponding molecular transitions are summarized in Table 1. To measure the tuning rate and the nonlinearity, we analyzed the etalon fringe spacings obtained from two parallel ZnSe plates as a function of voltage applied to the modulation input and then fitted with a quadratic function. Spectroscopic data, except for C_2H_2 (Ref. 6) and for NH_3,[7] were taken from the HITRAN 2000 database. For NH_3 and C_2H_2 the targeted absorption lines are close to the strongest in the NIR region, whereas the accessible CO_2 and H_2O lines are weak.

The power fluctuations of the laser output are 0.05% over a 20-ms time period. Slow drifts of 0.4% can occur on a longer time scale. To evaluate the frequency stability we used a reference cell filled with pure C_2H_2. The laser wavelength was adjusted to coincide with the steep slope of a C_2H_2 absorption line, which converts the frequency noise of the incident light into intensity noise of the transmitted light. Figure 2 depicts a 15-s record of the laser frequency, showing a maximum peak-to-peak variation of 150 MHz, with a -60-kHz/s drift over the 15-s record. The Doppler width of the CO_2 line (the heaviest molecule monitored in this study) is 360 MHz. Thus the laser frequency is sufficiently stable to keep the laser on the

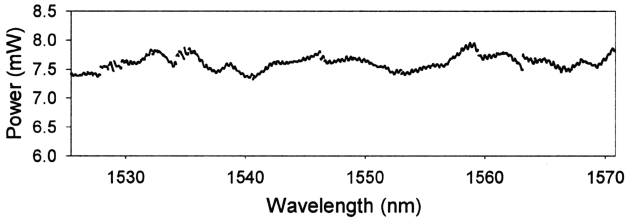

Fig. 1. Tunable diode laser power over the entire spectral tuning range.

0146-9592/04/161837-03$15.00/0

Table 1. Characteristics of the Four Laser Channels Used

Parameter	Laser Channel 02	08	12	14
Wave number (cm^{-1})	6514.2505	6528.7640	6529.1719	6541.2886
Wavelength in air (nm)	1534.64	1531.22	1531.13	1528.29
Laser power (mW)	6.97	7.00	7.00	7.08
Tuning rate (cm^{-1}/V)	0.383	0.499	0.462	0.403
Tuning nonlinearity (cm^{-1}/V^2)	-1.9×10^{-2}	-3.1×10^{-2}	-1.3×10^{-2}	-5.5×10^{-3}
Molecule	CO_2	NH_3	C_2H_2	H_2O
Line intensity [(cm^{-1}/molecule cm^{-2})]	1.90×10^{-24}	2.33×10^{-21}	1.22×10^{-20}	2.88×10^{-24}

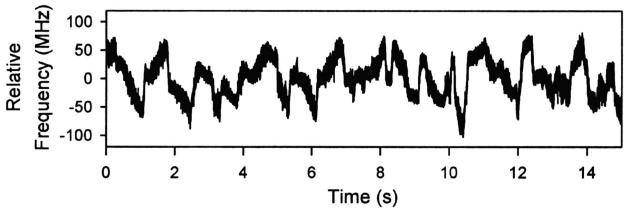

Fig. 2. Frequency fluctuations of the diode laser as a function of time.

absorption line without external frequency locking, especially if the lines are also pressure broadened at pressures of >80 Torr.

QEPAS is a novel alternative technique[3] to the traditional method of performing photoacoustic (PA) spectroscopy[8] in which the resonant acoustic signal buildup occurs in a high-Q piezoelectric crystal. A watch tuning fork (TF) is used as a QEPAS transducer. The two main advantages of QEPAS are its immunity to background acoustic noise and the small sample volume (ultimately <1 mm^3) required. The gas cell used in this research had a volume of ~1 cm^3.

The optical arrangement is depicted in Fig. 3. The laser beam is collimated by a 7-mm focal-length fiber collimator. A beam splitter (BS, an uncoated CaF_2, 30-arc min wedge) is used to reflect a part of the laser radiation to the photodiode (PD) through the reference gas cell, which allows for laser wavelength locking to the absorption line for improved long-term stability. Lens L, with a 36-mm focal length, focuses the laser light between the TF's prongs. The optical power in the QEPAS cell is ~75% of the collimator output power (7 mW) owing to Fresnel reflections. The beam passes through two 320-μm inner-diameter glass tubes of a 5-mm combined length acting as an acoustic resonator. These tubes are placed on both sides of the TF inside the cell and provide an enhancement factor of ~8 of the PA signal. The beam exiting the cell is directed to a pyroelectric detector for optical alignment and laser power monitoring. A mechanical chopper was added because the pyroelectric detector is not sensitive to constant irradiation. The laser is wavelength modulated at half of the TF's resonance frequency. The signal generated by the TF is amplified and demodulated at its resonance frequency, $f \sim 32{,}762$ Hz (second-harmonic detection) by a lock-in amplifier as described in Ref. 3. The lock-in amplifier's time constant was set to 1 s in these experiments.

The PA signal is directly proportional to the TF's Q factor and the molecular absorption and also depends on the vibrational–translational relaxation rate of the target transition.[9] Therefore the optimum operating pressure has to be determined for each gas and even for each selected transition. The TF's Q factor decreases with pressure approximately as a power function. At 30 Torr, $Q \sim 31{,}000$, whereas at 600 Torr it decreases to ~11,500. At the same time the peak absorption of any spectral line increases with pressure. For example, the NH_3 line listed in Table 1 has an absorption coefficient of 1.07×10^{-5} cm^{-1} at 50 Torr and reaches 1.8×10^{-5} cm^{-1} at 600 Torr, assuming a concentration of 1 part in 10^6 by volume (ppmv). The vibrational–translational relaxation rate also increases with pressure, which makes the process of acoustic generation more efficient. Because of these counteracting effects, there is an optimum pressure that yields the optimum detection sensitivity. This effect is illustrated in Fig. 4, which shows the PA signal versus the modulation width applied to the diode laser for a mixture of 1.4% of C_2H_2 in air. The six curves correspond to different pressures in the cell. It is evident from Fig. 4 that the optimum pressure is ~90 Torr, with a modulation width of 2 GHz. This optimum pressure value was verified to be optimum also for the CO_2, H_2O, and NH_3 transitions used in this study.

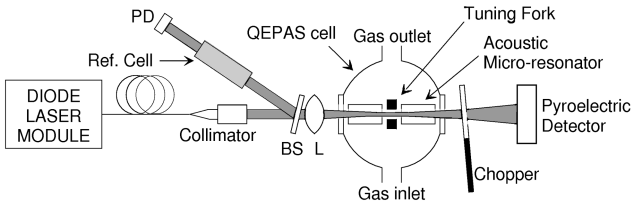

Fig. 3. Optical layout of a QEPAS-based gas sensor.

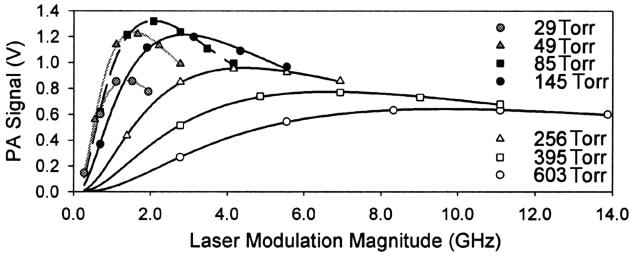

Fig. 4. Optimum working pressure for QEPAS monitoring of C_2H_2.

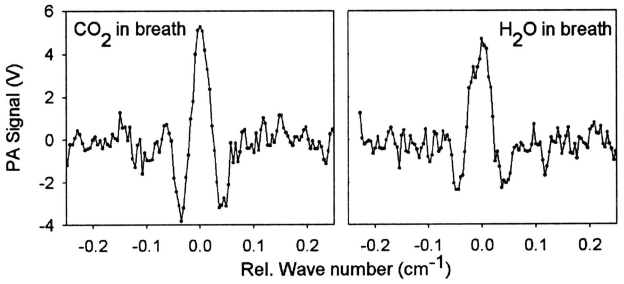

Fig. 5. QEPAS signal obtained during a frequency scan for the CO_2 and H_2O channels. A sample of exhaled human breath was analyzed. Line origins are listed in Table 1.

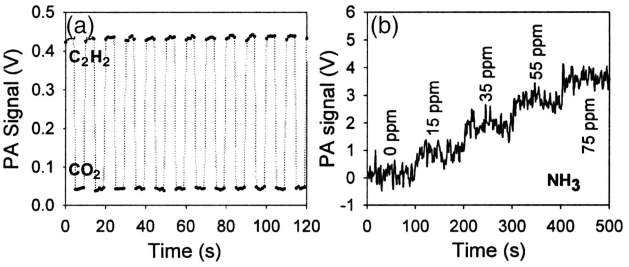

Fig. 6. (a) Simultaneous monitoring of 0.12% of C_2H_2 and CO_2 by laser channel switching. The black dots at the left reflect the PA signal; the lighter curve denotes the switching steps. (b) Monitoring of NH_3 in a flow configuration for several concentrations. Vertical scale, lock-in amplifier's output.

A human breath sample was used for a demonstration of simultaneous detection of H_2O and CO_2. In human breath the CO_2 concentration is ~5% and the humidity is close to 100%. The laser module was set to channel 02 (CO_2), a wavelength scan was performed, and the laser module was switched to channel 14 (H_2O) for a further wavelength scan. The resultant spectra are shown in Fig. 5. We evaluated the noise-equivalent sensitivity (NES) to be 10×10^{-9} cm^{-1} W^{-1} $Hz^{-1/2}$ for CO_2 and 8×10^{-9} cm^{-1} W^{-1} $Hz^{-1/2}$ for H_2O by measuring the standard deviation of the noise fluctuation that appeared on both sides of the absorption lines. The noise is not laser related, as it remained the same if the laser beam was blocked, but originates from the room-temperature thermal noise of the TF itself, which is the main sensitivity-limiting factor.

A mixture of 0.12% of C_2H_2 diluted in CO_2 was used for further demonstration of sensor performance. To record the QEPAS signals of both CO_2 and C_2H_2 we switched the laser from channel 02 to channel 12 every 5 s. No frequency sweep was applied. Instead, simultaneously with the laser channels, the modulation input voltage was switched between two constant voltages such that the laser frequency coincided with the top of the two gas lines. This technique proved to be an effective way to monitor two species at the same time, as can be seen from Fig. 6, left.

In another performance test, the ammonia concentration was monitored in flow conditions. We used a gas standard generator based on permeation tubes (Kin-Tek Model 491M) to produce a known adjustable concentration mixture of NH_3 in N_2 and thus to perform the QEPAS sensor calibration. In this test the diode laser's wavelength was locked to the absorption line as described in Ref. 3 (which was not possible for the weak lines of CO_2 and H_2O). Figure 6, right, depicts the PA signal recorded for four different NH_3 concentrations. The signal increases linearly with NH_3 concentration, with a 47 ± 2-mV/ppmv rate in terms of the lock-in amplifier's output. The projected zero level of the linear fit is 220 ± 60 mV, which we believe represents the real residual concentration of ~5 ± 2 ppm of NH_3 in the zero gas generator mode (wall desorption). A NES of 8×10^{-9} cm^{-1} W^{-1} $Hz^{-1/2}$ for a single measurement with a 1-s time constant was calculated by use of spectroscopic data for ammonia taken from Ref. 7 and the standard deviation of the PA signal.

In conclusion, a widely electrically tunable wavelength-programmable SG-DBR diode laser is an effective and convenient spectroscopic light source for multispecies gas monitoring. We evaluated the performance of the sensor by monitoring CO_2, C_2H_2, NH_3, and H_2O, using QEPAS. The achieved NES was $8–13 \times 10^{-9}$ cm^{-1} W^{-1} $Hz^{-1/2}$, which means that QEPAS now performs at a level close to that of traditional PA spectroscopy.[10]

We thank R. F. Curl for his most helpful advice and suggestions. The authors from Rice University also gratefully acknowledge financial support from NASA, the Robert Welch Foundation, the Texas Advance Technology Program, the National Science Foundation, the U.S. Office of Naval Research through a subaward from Texas A&M University, and Bacharach, Inc. D. Weidmann's e-mail address is weidmann@rice.edu.

References

1. L. Coldren, IEEE J. Sel. Top. Quantum Electron. **6,** 988 (2000).
2. B. L. Upschulte, D. M. Sonnenfroh, and M. G. Allen, Appl. Opt. **38,** 1506 (1999).
3. A. A. Kosterev, Y. A. Bakhirkin, R. F. Curl, and F. K. Tittel, Opt. Lett. **27,** 1902 (2002).
4. V. Jayaraman, D. A. Cohen, and L. A. Coldren, Appl. Phys. Lett. **60,** 2321 (2001).
5. J. Dunne, T. Farrell, and R. O'Dowd, in *Digest of Conference on Lasers and Electro-Optics* (Optical Society of America, Washington, D.C., 1999), pp. 147–148.
6. S. L. Gilbert and W. C. Swann, NIST Spec. Publ. **260-133** (2001).
7. M. E. Webber, D. S. Baer, and R. K. Hanson, Appl. Opt. **40,** 2031 (2001).
8. A. Miklós, P. Hess, and Z. Bozóki, Rev. Sci. Instrum. **72,** 1937 (2001).
9. A. A. Kosterev, Y. A. Bakhirkin, F. K. Tittel, S. Blaser, Y. Bonetti, and L. Hvozdara, Appl. Phys. B **78,** 673 (2004).
10. M. B. Pushkarsky, M. E. Webber, and C. K. N. Patel, Appl. Phys. B **77,** 381 (2003).